Amino-functionalized SBA-15 type mesoporous silica having nanostructured hexagonal platelet morphology†

Sujandi,[a] Sang-Eon Park,*[a] Dae-Soo Han,[a] Sang-Cheol Han,[a] Myung-Jong Jin[b] and Tetsu Ohsuna[c]

Received (in Cambridge, UK) 14th June 2006, Accepted 9th August 2006
First published as an Advance Article on the web 23rd August 2006
DOI: 10.1039/b608463j

Amino-functionalized SBA-15 type mesoporous silicas having unique hexagonal platelet morphologies with short channels (100–300 nm) running parallel to the thickness of the nanostructured hexagonal platelet type morphologies have been directly synthesized by co-condensation of aminopropyltriethoxysilane (APTES) and sodium metasilicate as a silica source in the presence of Pluronic P123 triblock copolymer as a structure directing agent.

In recent years the challenges in the study of mesoporous materials have been focused on the materials practical application to catalysis, separation, sensor, drug delivery, *etc.* by both incorporation of organic functionality through inorganic–organic hybridization and morphology and pore structure controls.[1,2] In this context, the morphologically controlled synthesis of organo-functionalized large pore mesoporous materials such as SBA-15 with high structural regularity is considered as one of the strategies.[2] However, so far only purely silicious SBA-15 materials with different well-defined morphologies have been synthesized by the addition of co-surfactants, additives, or co-solvents during the synthesis.[3] On the other hand, the addition of organosilanes during the direct synthesis of organo-functionalized SBA-15 mesoporous materials in strongly acidic conditions mostly resulted in materials with poor textural morphologies.[4]

Amino-functionalized mesoporous materials have received considerable attention in recent years among the variety of organo-functionalized mesoporous materials synthesized through the direct synthesis route. Indeed, it is a particularly useful functionality for many practical applications such as heterogeneous base catalysis, toxic arsenate ion trapping, biomolecule immobilization, as covalent spacer in the immobilization of catalytically active metal complexes, and as supports for metallic nanoparticles.[5] However, highly ordered large pore amino-functionalized mesoporous materials are perhaps the most difficult derivatives to synthesize using a direct synthesis approach in the presence of non-ionic surfactants as structure directing agents.[4] The obtained materials were known to lack uniformity and controlled mesoporosity and also were mostly obtained in a fibrous morphology handicapped with poor dispersion and pore accessibility.

Here, we report morphologically controlled amino-functionalized SBA-15, synthesized directly from the co-condensation of sodium metasilicate and aminopropyltriethoxysilane (APTES) in the presence of P123 triblock copolymer as a structure directing agent under strongly acidic conditions. Microwave irradiation was applied as a heating source throughout the hydrothermal aging treatment in order to achieve the potential advantages of microwave synthesis such as rapid and homogeneous heating, homogeneous nucleation and rapid crystallization, phase selectivity, and facile particle size and morphological control.[6] Our results showed that highly ordered amino-functionalized SBA-15 materials having short channels in the submicron range and uniform particle sizes in hexagonal prism and hexagonal platelet morphologies could be synthesized by using inexpensive sodium metasilicate as a silica source instead of TEOS (tetraethoxysilane) without either protecting the amino group of APTES[6] or prehydrolysis of the silica source[7] (ESI†).

Fig. 1 shows the small-angle X-ray diffraction patterns of the amino-functionalized SBA-15 which were synthesized by co-condensation under microwave irradiation with different amine to silica molar ratios in the initial synthesis mixtures. The XRD patterns showed well-resolved peaks with very intense diffraction peaks at $2\theta = 0.8$–0.9° and two or more peaks at higher degrees, which were indexed to the 100, 110, 200, 300 and 220 planes characteristic of the long range order and excellent textural uniformity of SBA-15 mesoporous material with a mesostructure of hexagonal space group symmetry *P6mm*. The XRD main peak intensity of NH_2pr(10)-SBA-15 is weaker and only the 110 and 200 diffraction peaks are well-resolved at the higher degree.

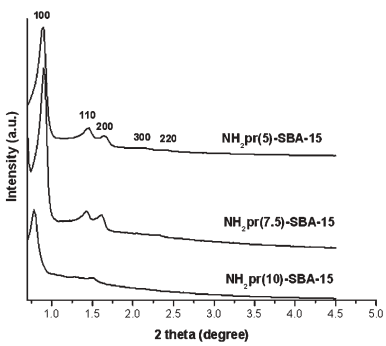

Fig. 1 Small-angle X-ray diffraction patterns of NH_2pr(x)-SBA-15 with x = NH_2 to SiO_2 molar ratio in the initial synthesis mixtures (see Experimental section in ESI†).

[a]*Laboratory of Nano-Green Catalysis, Nano Center for Fine Chemicals Fusion Technology, Department of Chemistry, Inha University, Incheon, 402-751, Korea. E-mail: separk@inha.ac.kr; Fax: +82 32 867 5604; Tel: +82 32 860 7675*
[b]*Department of Chemical Engineering, Inha University, Incheon, 402-751, Korea*
[c]*Japan Science and Technology Agency (JST) and Kagami Memorial Laboratory for Materials Science and Technology, Waseda University[3], Japan*
† Electronic supplementary information (ESI) available: Experimental and characterization details. See DOI: 10.1039/b608463j

The mesoporosity of the samples was characterized by using a nitrogen sorption analysis. The N_2 adsorption–desorption isotherms (ESI†) for all samples showed type IV isotherms with H1-type hysterisis loops which were typical for mesoporous materials having cylindrical type mesostructures. The sharp steep increases in the adsorptions at P/P_0 = 0.7–0.8 implied that the materials posses large pore sizes with narrow distributions.[8] This was confirmed by the pore size distributions calculated using a BJH (Barrett, Joyner and Halenda) method from the adsorption branches, which exhibited narrow pore distributions with maxima between 9 and 11 nm.

The SEM images (Fig. 2) revealed that the directly synthesized amino-functionalized SBA-15 mesoporous samples from the co-condensation reactions between APTES and sodium metasilicate under microwave irradiation have uniform particle sizes with hexagonal prism and platelet morphologies when the amine to silica molar ratio in the initial synthesis mixtures is set at 5% or higher. Addition of a small amount of APTES (3%) to the initial reaction mixture resulted in a fibrous-like morphology with connected rod-like particles as in the case of ordered SBA-15. Addition of larger amounts of APTES such as 5% gave a stacked hexagonal prism-like morphology and when 7.5% and 10% APTES were added, the morphologies were hexagonal disk-like and hexagonal chip-like, respectively. Therefore, the amounts of APTES in the initial reaction mixtures were definitely controlling the morphologies of the amino-functionalized SBA-15.

The HR-TEM analyses indicated that the materials have highly ordered 1D mesopore structures with a 2D hexagonal arrangement. The TEM images also clearly showed that the materials have very short 1D mesopore channels of submicrometer length (100–300 nm). The channel directions of the 2D-hexagonal structures are parallel to the thickness direction of the hexagonal platelet morphologies (Fig. 3). From the SEM and HR-TEM analyses, the channel length of NH_2pr(5)-SBA-15, having hexagonal prism-like morphology with a particle size within 1–2 μm, could be estimated within the range of 200–300 nm. Whereas NH_2pr(7.5)-SBA-15, with hexagonal disk-like morphology, and NH_2pr(10)-SBA-15, with hexagonal chip-like morphology, have wider (001) hexagonal plates (5–6 μm) with shorter 1D mesopore channels *i.e.* within 100–200 nm.

The addition of APTES to the synthesis mixture of NH_2pr(x)-SBA-15 under strongly acidic conditions apparently affects the formation of not only the mesoscopic structure but also the macroscopic morphology. The addition of larger amounts of APTES to the reaction mixtures, resulted in the more positively

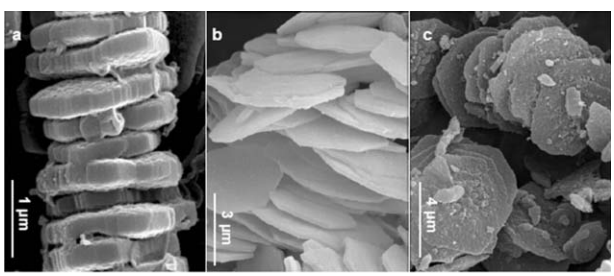

Fig. 2 SEM images of amino-functionalized SBA-15 with different NH_2 : SiO_2 molar ratios in the initial synthesis mixtures: (a) NH_2pr(5)-SBA-15; (b) NH_2pr(7.5)-SBA-15; and (c) NH_2pr(10)-SBA-15.

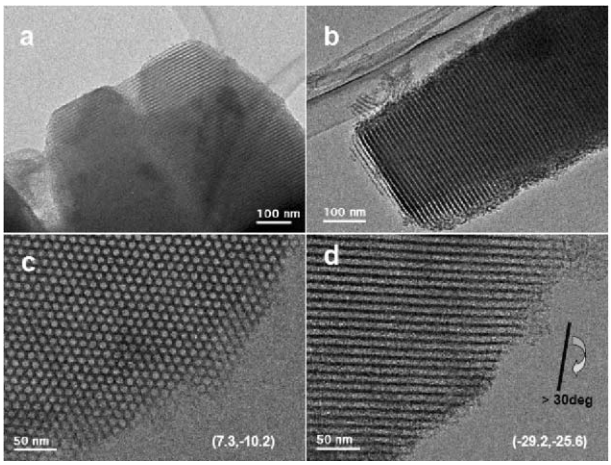

Fig. 3 TEM images of amino-functionalized SBA-15 with different NH_2 : SiO_2 molar ratios in the initial synthesis mixtures: (a) NH_2pr(5)-SBA-15; (b) NH_2pr(7.5)-SBA-15; (c) NH_2pr(10)-SBA-15; and (d) image obtained after specimen c is tilted by more than 30°.

charged APTES being dispersed at the end of the silicatropic rod-like micelle and caused the passivation of the end-to-end silicate–micelle anchoring along the longitudinal axis due to charge repulsion. The amine groups might also contribute to the diminution of the number of hydroxyl groups which are essential for the end-to-end anchoring. Hence, the growth of mesostructured silica along the longitudinal axis was unable to proceed for a longer time than for the growth along the transverse axis. This was ascribed to the formation of the wider hexagonal platelet type morphology with shorter channels.[9] The use of sodium metasilicate was also crucial in this observation, since the co-condensations between TEOS and APTES in a strongly acidic solution in the presence of P123 surfactant were not successful in obtaining the ordered mesoporous silicas without TEOS pre-hydrolysis or protecting the amino group of APTES. The *in-situ* generated NaCl salt seemed to contribute to strengthening the interaction among the silicate species, protonated APTES, and the surfactant hydrophilic head groups and to decreasing the critical micelle concentration (CMC).[10]

The ^{13}C solid state NMR spectroscopy and NIR spectra (ESI†) provided clear evidence that the aminopropyl group was indeed functionalized as intended. The ^{13}C CP/MAS NMR spectrum of surfactant free NH_2pr(7.5)-SBA-15 displayed three peaks at 8.1, 23.7 and 42.4 ppm which were assigned to the carbon atoms of the tethered aminopropyl group.[7] The NIR spectra revealed vibration bands that correspond to primary amine at 2022 and 1530 nm. The former band could be assigned to the combination ($\delta + \nu$) of primary amine stretching and bending vibration modes and the latter could be assigned to the overtone (2ν) of the primary amine stretching vibration band, respectively.[11] The amounts of incorporated aminopropyl groups in the obtained samples were estimated based on CHN elemental analysis. The elemental analysis showed that the amounts of tethered aminopropyl groups were close to the calculated values based on the APTES concentrations in the initial reaction mixtures.

In order to check the accessibility and the state of the tethered aminopropyl functional groups, the benzaldehyde and di-*tert*-butylsalicylaldehyde adsorptions were inverstigated. Fig. 4 shows

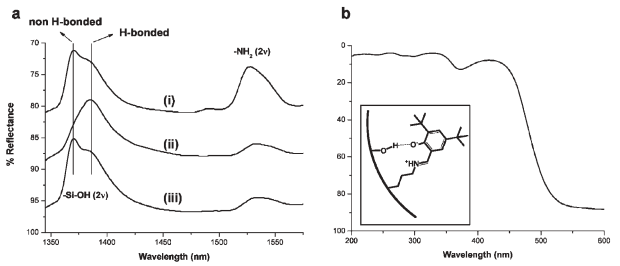

Fig. 4 (a) NIR spectra of NH_2pr(7.5)-SBA-15: (i) before adsorption, (ii) after *tert*-butylsalicylaldehyde adsorption, and (iii) after benzaldehyde adsorption. (b) UV-Vis spectrum of NH_2pr(7.5)-SBA-15 after *tert*-butylsalicylaldehyde adsorption (Insert: the proposed structure of the zwitterionic species). Reaction conditions: 1 mmol of substrate was introduced into the stirred suspension of 0.5 g catalyst in 10 ml toluene and the final mixture was stirred for at least 4 h at room temperature.

the NIR and UV-Vis DRS (depolarized Rayleigh spectrum) spectra of the NH_2pr(7.5)-SBA-15 sample after adsorption. The UV-Vis DRS of the sample after adsorption with di-*tert*-butylsalicylaldehyde showed a strong band at 423 nm, which was due to the formation of zwitterionic species on the silica surface in which the phenolic oxygen is H-bonded to the surface silanol group (Fig. 4b).[12] Therefore, the changes in the intensity of the NIR bands corresponding to the first overtone of the surface silanol groups stretching vibration mode upon the *tert*-butylsalicylaldehyde adsorption *i.e.* decrease for the non-H-bonded (1370 nm) and increase in the H-bonded (1385 nm) surface silanol groups vibration bands, respectively, suggested that the aminopropyl moieties before adsorption were mostly in the non-H-bonded state pendant to the surface.[13] If this was not the case, those changes should be observed upon benzaldehyde adsorption (see Fig. 4a). However, as shown in Fig. 4a(iii), the NIR spectrum of the benzaldehyde adsorbed sample showed that the band intensities for both non-H-bonded and H-bonded bands were similar to the band intensities of the sample before adsorption. Based on the GC analysis of the remaining benzaldehyde in solution after the adsorption, it could be estimated that the accessible aminopropyl group was 0.99 mmol g^{-1} or 85% of the total incorporated aminopropyl group in the sample.

Amino-functionalized mesoporous materials have been widely applied in base-catalyzed condensation reactions such as Knoevenagel, Claisen–Schmidt, and aldol condensations. In order to investigate the catalytic activity of the tethered aminopropyl groups as well as the potential application of the mesopore short channels in catalysis, the obtained amino-functionalized SBA-15 sample was tested as a solid-base catalyst in a liquid-phase Knoevenagel condensation between benzaldehyde and ethyl cyanoacetate. Fig. 5 shows the time-course for the Knoevenagel condensation of benzaldehyde (1) with ethyl cyanoacetate (2) catalyzed by NH_2pr(7.5)-SBA-15. The amounts of substrate introduced into the reaction system were varied from 1.5 mmol to 6 mmol. All the reactions exhibited near 100% selectivity for ethyl cyanocinnamate (3) and showed excellent activities giving turnover frequencies (TOF) of $\sim$120 h^{-1}. No serious diffusion or mass transfer limits were observed, especially when the amounts of 1 and 2 were set to 1.5 mmol in which the reaction was nearly completed in such a short period time (10 min). The high activity

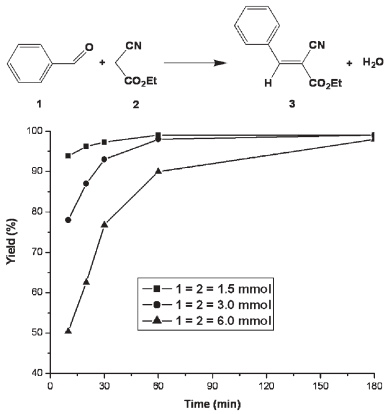

Fig. 5 Time-course of the Knoevenagel condensation of benzaldehyde (1) with ethyl cyanoacetate (2) catalyzed by NH_2pr(7.5)-SBA-15. Reaction was carried out with 50 mg of catalyst in 1 ml of toluene at 30 °C.

of the tethered aminopropyl moieties in the base-catalyzed reaction could also result from it's high dispersion and non-H-bonded state.[13]

This work was supported by KOSEF A3 Foresight Program (33426-1).

Notes and references

1 S. H. Tolbert, A. Firouzi, G. D. Stucky and B. F. Chmelka, *Science*, 1997, **278**, 264; J. Y. Ying, C. P. Mehnert and M. S. Wong, *Angew. Chem., Int. Ed.*, 1999, **38**, 56; A. Stein, B. J. Melde and R. C. Schroden, *Adv. Mater.*, 2000, **12**, 1403; M. E. Davis, *Nature*, 2002, **417**, 813; J. Kim, J. E. Lee, J. Lee, J. H. Yu, B. C. Kim, K. An, Y. Hwang, C.-H. Shin, J.-G. Park, J. Kim and T. Hyeon, *J. Am. Chem. Soc.*, 2006, **128**, 688.

2 C. Thoelen, J. Paul, I. F. J. Vankelecon and P. A. Jacobs, *Tetrahedron: Asymmetry*, 2000, **11**, 4819; J. Fan, J. Lei, L. Wang, C. Yu, B. Tu and D. Zhao, *Chem. Commun.*, 2003, 2140; S. Huh, J. W. Wiench, J.-C. Yoo, M. Pruski and V. S.-Y. Lin, *Chem. Mater.*, 2003, **15**, 4247; C. Boissière, M. Kümmel, M. Persin, A. Larbot and E. Prouzet, *Adv. Funct. Mater.*, 2001, **11**, 129.

3 D. Zhao, J. Sun, Q. Li and G. D. Stucky, *Chem. Mater.*, 2000, **12**, 275; C. Yu, J. Fan, B. Tian and D. Zhao, *Chem. Mater.*, 2004, **16**, 889; Z. Kónya, J. Zhu, A. Szegedi, I. Kiricsi, P. Alivisatos and G. A. Somorjai, *Chem. Commun.*, 2003, 314; H. Zhang, J. Sun, D. Ma, X. Bao, A. Klein-Hoffmann, G. Weinberg, D. Su and R. Schölgl, *J. Am. Chem. Soc.*, 2004, **126**, 7440.

4 A. S. Maria and X. S. Zhao, *J. Phys. Chem. B*, 2003, **107**, 12650; X. Wang, J. Shah, S.-S. Kim and T. J. Pinnavaia, *Chem. Commun.*, 2004, 572.

5 A. Mehdi, C. Reyé, S. Brandès, R. Guilard and R. J. P. Corriu, *New J. Chem.*, 2005, **29**, 965.

6 Y. K. Hwang, J.-C. Chang, S.-E. Park, D. S. Kim, Y.-U. Kwon, S. H. Jhung, J.-S. Hwang and M. S. Park, *Angew. Chem., Int. Ed.*, 2005, **117**, 562; Y. K. Hwang, J.-S. Chang, Y.-U. Kwon and S.-E. Park, *Microporous Mesoporous Mater.*, 2004, **68**, 21.

7 X. Wang, K. S. K. Lin, J. C. C. Chan and S. Cheng, *J. Phys. Chem. B*, 2005, **109**, 1763.

8 D. Zhao, Q. Huo, J. Feng, B. F. Chmelka and G. D. Stucky, *J. Am. Chem. Soc.*, 1998, **120**, 6024.

9 X. Y. Bao and X. S. Zhao, *J. Phys. Chem. B*, 2005, **109**, 10727.

10 C. Yu, B. Tian, J. Fan, G. D. Stucky and D. Zhao, *Chem. Commun.*, 2001, 2726.

11 L. Xu, H. Fu and J. R. Schlup, *J. Am. Chem. Soc.*, 1994, **116**, 2821.

12 J. D. Bass, A. Solovyov, A. J. Pascall and A. Katz, *J. Am. Chem. Soc.*, 2006, **128**, 3737.

13 T. Yokoi, H. Yoshitake, T. Yamada, Y. Kubota and T. Tatsumi, *J. Mater. Chem.*, 2006, **16**, 1125.